



Numerical simulation on the falling film absorption process in a counter-flow absorber

Shoushi Bo, Xuehu Ma*, Zhong Lan, Jiabin Chen, Hongxia Chen

Institute of Chemical Engineering, Dalian University of Technology, 158# Zhongshan Road, Dalian 116012, China

ARTICLE INFO

Article history:

Received 25 October 2008

Received in revised form 20 April 2009

Accepted 21 April 2009

Keywords:

Falling film absorption
Heat and mass transfer
Numerical simulation

ABSTRACT

Falling liquid film is commonly employed in variety of industrial systems, such as LiBr/H₂O absorption heat pump or chiller. In this paper, the falling film absorption in aqueous lithium bromide solution was investigated numerically using CFD software package-Fluent. The practical convective boundary condition at the cooling water side was considered. The heat transfer coefficient is assumed constant, and the coolant temperature changes linearly along its flow path. The numerical results indicate that the profile of temperature is exponential and their gradients are high due to the distinct heat effect associated with the absorption at the interface and the cooling effect of coolant at the wall at small downstream distance. As the downstream distance increases, the profile of temperature is nearly linear. The absorption heat and mass fluxes reach a maximum at the inlet region and decrease at the outside of the inlet region. Specially, the effect of variable physical properties on the absorption process was considered and discussed. The prediction of the total absorption mass transfer rate is about 6.5% higher when assuming constant properties.

© 2009 Elsevier B.V. All rights reserved.

1. Introduction

The LiBr/H₂O absorption heat pump or chiller is gaining global acceptance as one promising candidate for waste heat recovery. The performance of absorber is critical to the overall performance, size, and first-cost of the heat pump or chiller system. The design of the absorber incorporates the heat and mass transfer of falling liquid film. So to proceed adequately in the development of absorption heat pumps or chillers, a better understanding is required of the combined heat and mass transfer process in absorption of LiBr/H₂O.

In the case of falling film absorption, a simultaneous heat and mass transfer dominates the performance. As absorption occurs, heat and mass are transferred through the interface and within the liquid phase. The exchange of mass across the liquid–vapor interface involves the generation of heat. The heat effect associated with this mass exchange increases the liquid temperature at the interface accordingly, which consequently influences the equilibrium states of pressure and concentration and in turn affects the mass transfer. Furthermore the driving forces for heat and mass transfer change as the process progresses both due to the variation of the local temperature, concentration gradients and the interfacial equi-

librium condition. In addition, the falling film flow regimes make the absorption more complicated.

Normally, the analysis of combined heat and mass transfer is performed based on the governing equations of continuity, diffusion and energy. Grigoréva and Nakoryakov [1] and Grossman [2] modeled and analyzed the absorption in laminar falling films using Fourier separation of variables techniques. They analytically solved the energy and species equations for the heat and mass transfer to a laminar falling film having constant temperature or adiabatic wall boundary condition. But Grigoréva and Nakoryakov [1] and Grossman [2] adopted different velocity profiles. Brauner et al. [3] proposed an improvement for the cases where the absorbate concentration is comparable to that of the absorbent. Van der Wekken and Wassenaar [4] presented the heat transfer model to a constant temperature coolant, and use the coolant heat transfer coefficient as a variable to study the heat and mass transfer process. Habib and Wood [5] formulated a model for co-current absorption on a laminar, vertical film considering the heat and momentum transfer in the vapor phase. Yang and Wood [6] numerically studied the case of inlet solution temperature different from the temperature of wall on laminar falling film absorption. Kawae et al. [7] investigated the effect of the physical properties of LiBr solutions. Yoon et al. [8] focused on the numerical study in absorption of vertical plate absorber which was cooled by water, and the temperature of cooling water is assumed to change linearly. Yigit [9] investigated the falling film absorption on a vertical tube. Morioka and Kiyota [10], Yang and Jou [11], Patnaik [12], Sabir et al. [13] conducted

* Corresponding author. Tel.: +86 411 83653402; fax: +86 411 83653402.
E-mail address: xuehuma@dlut.edu.cn (X. Ma).

Nomenclature

C	LiBr concentration (wt.%)
C_p	specific heat ($\text{J kg}^{-1} \text{K}^{-1}$)
D	diffusion coefficient ($\text{m}^2 \text{s}^{-1}$)
g	gravitational acceleration (m s^{-2})
H	enthalpy (kJ kg^{-1})
H_a	heat of absorption (kJ kg^{-1})
h_c	coolant heat transfer coefficient ($\text{W m}^{-2} \text{K}^{-1}$)
k	thermal conductivity ($\text{W m}^{-1} \text{K}^{-1}$)
L	plate height (m)
m	mass flux ($\text{kg m}^{-2} \text{s}^{-1}$)
P	absorption pressure (kPa)
q	heat flux (W m^{-2})
Re	Reynolds number
T	temperature (K or $^{\circ}\text{C}$)
u	velocity in x -direction (m s^{-1})
U	average velocity (m s^{-1})
v	velocity in y -direction (m s^{-1})

Greek symbols

α	thermal diffusivity ($\text{m}^2 \text{s}^{-1}$)
δ	liquid film thickness (m)
μ	dynamic viscosity (Pa s)
ρ	density (kg m^{-3})
Γ	spray density ($\text{kg m}^{-1} \text{s}^{-1}$)
ε	absorption coefficient

Subscripts

1	solid LiBr
2	H_2O
b	bulk
c	cooling water
in	inlet
i	liquid–vapor interface
min	minimum value at the outlet
out	outlet
s	absorption solution
w	plate wall

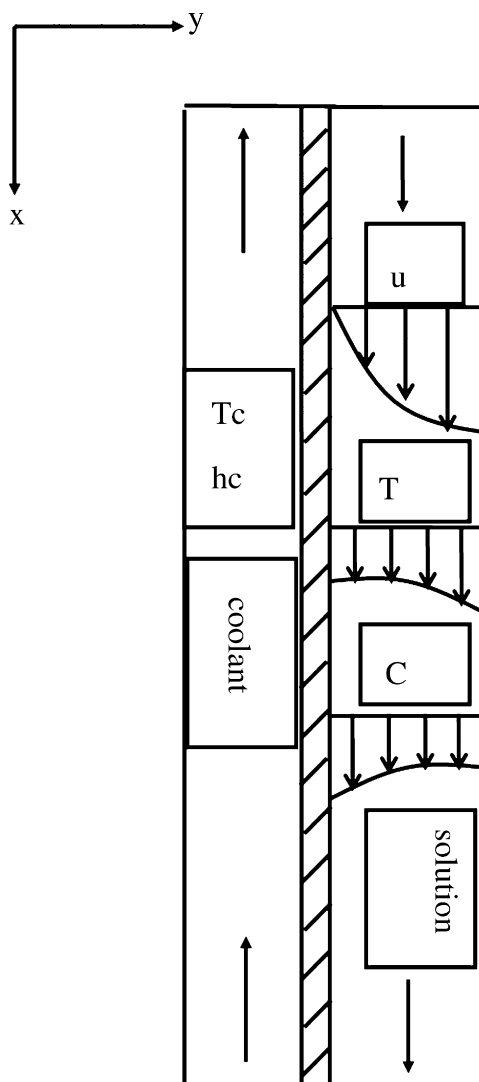


Fig. 1. Schematic diagram of falling film absorption system.

analytical studies of the wavy-laminar problem. Grossman and Heath [14] extended the falling film analysis of film absorption to turbulent flow. In the aforementioned analysis most researchers assumed the constant physical properties.

The present work numerically simulated the heat and mass transfer during the absorption process of LiBr–water liquid film falling outside a vertical tube using CFD software-Fluent. The practical convective boundary condition at the cooling water side was considered. The coolant heat transfer coefficient is assumed constant and the coolant temperature changes linearly along its flow path, which is validated experimentally by Miller [15].

2. Governing equations and boundary conditions

The system analyzed in the present study is depicted schematically in Fig. 1. A film of liquid solution, composed of absorbent (LiBr) and absorbate (water), flows downward outside a vertical tube. LiBr always remains in the liquid phase, and steam is absorbed into the solution. The film is in contact with stagnant steam at constant pressure. At the entrance, the liquid solution is at a predefined temperature and concentration corresponding to three states: slightly superheated, slightly subcooled and equilibrium. Coolant usually flows countercurrent to the falling liquid film, and the integrated heat and mass transfer process occurred in the absorber as the

falling film of strong solution absorbs steam. The LiBr solution has a vapor pressure lower than absorbate vapor pressure. As a result of this difference, absorption occurs. The water absorbed at the interface diffuses into the film. Simultaneously thermal effect associated with absorption boosts the liquid temperature near the interfacial region, improving the heat transfer within liquid film. Meanwhile, the liquid film is cooled by cooling water flowing inside the tube. Because the liquid film thickness generally is less than 1% of tube diameter under the practical conditions, a two-dimensional Cartesian coordinate system was chosen. In Fig. 1 coordinate x is in the streamwise direction and coordinate y is normal to the wall.

The following assumptions have been made in formulating the model:

- (1) The physical properties of the liquid solution are constant and independent of temperature and concentration (the effect of variable properties will be considered in the last section).
- (2) Thermodynamic equilibrium exists at the interface.
- (3) Heat transfer in the vapor phase is negligible compared to that in the liquid phase.
- (4) Liquid is postulated as Newtonian. Fluid flow is 2D laminar, full developed and non-wavy throughout.
- (5) No shear forces are exerted on the liquid by vapor.

- (6) The mass rate of vapor absorbed is very small compared to the solution flow rate so that the film thickness and flow velocities can be considered as constant.
- (7) The cooling water is countercurrent with respect to the flow of liquid film and its temperature changes linearly.
- (8) The coolant heat transfer coefficient remains constant. The thermal resistance of the solid wall is negligible.

Under the above assumptions, the 2D energy and diffusion equations could be reduced as

$$\rho c_p \left(u \frac{\partial T}{\partial x} + v \frac{\partial T}{\partial y} \right) = k \left(\frac{\partial^2 T}{\partial x^2} + \frac{\partial^2 T}{\partial y^2} \right) + \frac{\partial}{\partial y} \left(\sum_{i=1}^2 \rho D_i \frac{\partial C_i}{\partial y} H_i \right) \quad (1)$$

$$u \frac{\partial C}{\partial x} + v \frac{\partial C}{\partial y} = D \left(\frac{\partial^2 C}{\partial x^2} + \frac{\partial^2 C}{\partial y^2} \right) \quad (2)$$

The second term at the right hand side of Eq. (1) denotes the change in energy due to inter-diffusion, which is retained in the governing energy equations. Where ρ is the solution density, c_p is the specific heat, k is thermal conductivity, D is diffusion coefficient. The symbol H is enthalpy and subscripts 1 and 2 denote LiBr and H_2O , respectively.

According to the Nusselt theory, transverse velocity v is zero and the downstream velocity profile u is parabolic as a function of y and is given as follows:

$$u = \frac{3}{2} U \left(2 \frac{y}{\delta} - \left(\frac{y}{\delta} \right)^2 \right), \quad (3)$$

where

$$U = \frac{\Gamma}{\rho \delta}, \quad \delta = \left(\frac{3 \Gamma \mu}{\rho^2 g} \right)^{1/3} \quad (4)$$

The following boundary conditions for temperature and concentration are applied:

- (1) At the entrance, the uniform liquid film temperature and concentration can be assumed, and LiBr solution is in thermodynamic equilibrium state:

$$T = T_{s,in}, \quad C = C_{s,in}, \quad (5)$$

- (2) At the wall, it is impermeable, thus the gradient of concentration is equal to zero. For the wall temperature, the third boundary condition is given in term of coolant temperature and coolant heat transfer coefficient. The cooling water is countercurrent with respect to the flow of liquid film and its temperature changes linearly. The coolant heat transfer coefficient remains constant:

$$\frac{\partial C}{\partial y} = 0, \quad k \frac{\partial T}{\partial y} = h_c (T_w - T_c). \quad (6)$$

- (3) At the interface, the LiBr solution is in its saturation state. The local interfacial absorption heat flux is described as [16]:

$$C_i = C_i(T_i, P), \quad k \frac{\partial T}{\partial y} = D \cdot \rho \frac{\partial C}{\partial y} \cdot H_a = q \quad (7)$$

- (4) At the outlet, the type of outflow boundary condition is adopted, where the exit flow is assumed to be close to a fully developed condition

$$\frac{\partial T}{\partial x} = 0, \quad \frac{\partial C}{\partial x} = 0. \quad (8)$$

3. Solution method

The CFD software, Fluent, was used to simulate the heat and mass transfer in falling film absorption process. Fluent uses a

control-volume-based technique to convert the governing equation to algebraic equations. Second order upwind discretization scheme was used to discretize the governing Eqs. (1) and (2). In the present simulation, the computational domain is adopted to a fixed rectangular domain. The film flowing distance is 1 m. The film thickness is dependant on Re . The mesh number is 30×3000 in x and in y . The convergence criterion for diffusion equation is 1×10^{-4} , and the convergence criterion for energy equation is 1×10^{-7} .

4. Results and discussion

4.1. Validity of the model

The validity of the model was verified with the comparison of the calculated interfacial temperature and concentration with the results of Kawae [7] under the same conditions, as shown in Fig. 2. It can be seen that the present results agree very well with those of Kawae [7].

The present study was performed under more practical conditions. The inlet strong solution corresponds to equilibrium states and coolant heat transfer coefficient is considered to be constant. Operating conditions are listed in Table 1, and physical properties of LiBr solution are collected from Ref. [8]. The heat and mass transfer characteristics of falling film shown in Figs. 3–5 are the results for cases of constant coolant heat transfer coefficient of $2000 \text{ W m}^{-2} \text{ K}^{-1}$ and constant physical properties. Fig. 6 shows the effect of variable properties on the temperature and concentration profiles. The effect of variable properties on typical local interfacial heat flux and mass flux along the wall is plotted in Fig. 7.

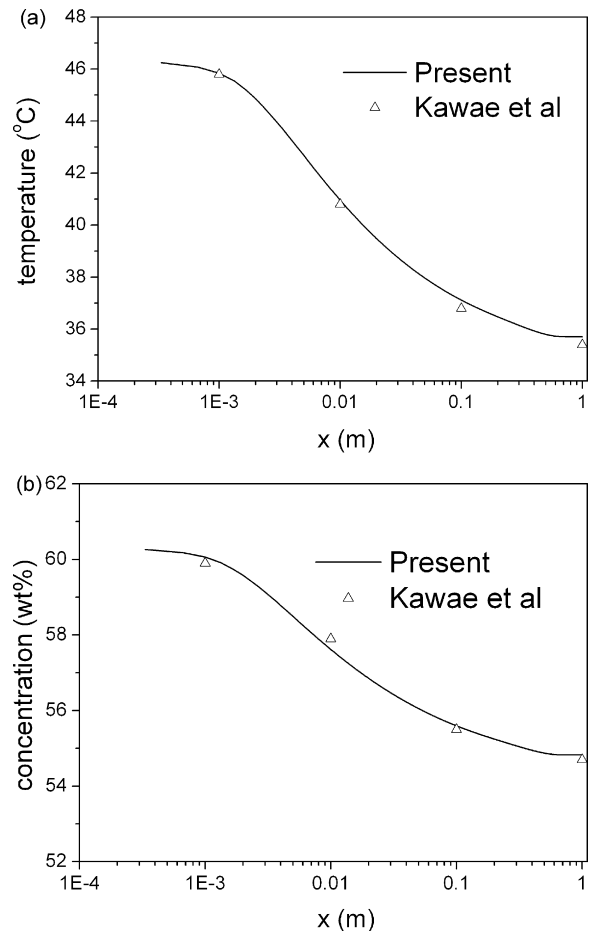


Fig. 2. Comparison of the present results with data in the literature (a) interfacial temperature and (b) interfacial concentration.

Table 1
Operation conditions.

Operating parameter	Values
$T_{s,in}$ (°C)	46.5
$C_{s,in}$ (wt.%)	60.38
$T_{c,in}$ (°C)	32
$T_{c,out}$ (°C)	36
h_c ($W m^{-2} K^{-1}$)	2000
L (m)	1
P (kPa)	1
Γ ($kg m^{-1} s^{-1}$)	0.0142

4.2. Temperature and concentration profiles

Fig. 3 describes the typical temperature and concentration profiles at different downstream positions. The abscissa is dimensionless film thickness. $y/\delta = 0$ and $y/\delta = 1$ denote the locations of wall and interface, respectively. It should be noted from Fig. 3(a) that at small downstream distance ($x = 0.005$ m), the profile of temperature is exponential, and their gradients are high due to the distinct heat effect associated with the absorption at interface and the cooling effect of coolant at the wall, as shown in Fig. 5(b). As the downstream distance increases, the heat transfer fluxes at the interface and wall decrease and the profile of temperature is nearly linear. It can be concluded that the heat conduction dominates in the liquid film far downstream from the inlet. This may be also explained as the variation of the magnitude of absorption heat at the interface, which can be considered as the energy source term of the conduction heat transfer within the liquid film, as shown in Fig. 5(b). For the concentration profile in Fig. 3(b), it can be seen that the majority of mass diffusion takes place in a thin layer near

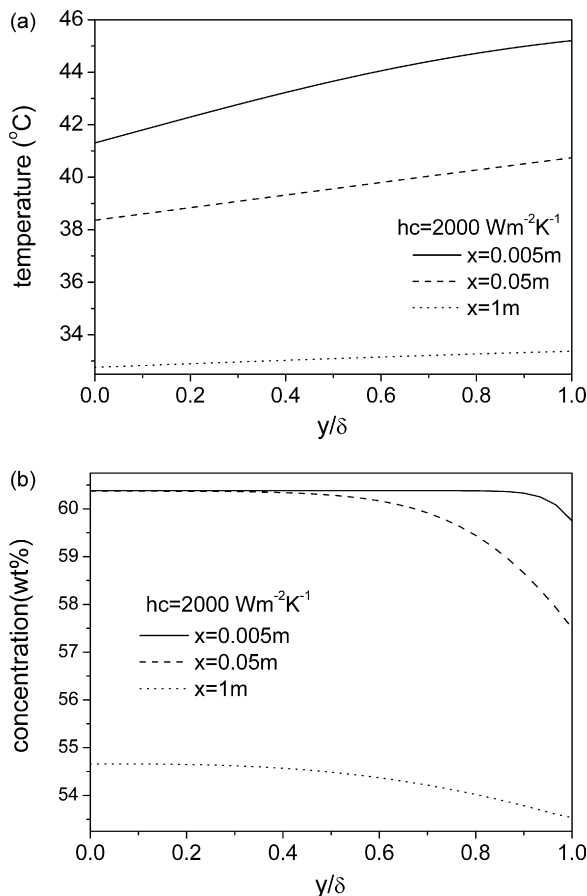


Fig. 3. The profile across the film: (a) temperature and (b) concentration.

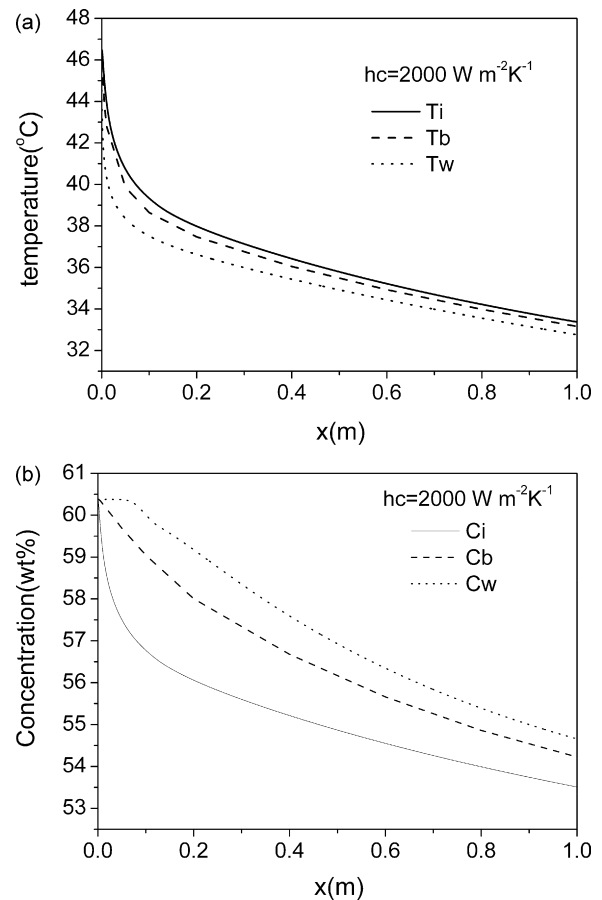


Fig. 4. The profile along the wall: (a) temperature and (b) concentration.

the liquid–vapor interface within a small distance in x direction. As the downstream increases, the mass diffuses further towards the wall, and causes the variation of concentration at the wall. For a LiBr–water system, the Le number ($Le = \alpha/D$) is on the order of 10^2 . Thus the diffusion boundary layer develops slowly compared to the thermal boundary layer, and resulting in the temperature profile development faster than the concentration profile, as shown in Fig. 3(a) and (b).

Fig. 4 shows the variation of typical temperature and concentration profiles with the downstream flowing distance. Initially, the changes of liquid temperature at interface, bulk and wall are remarkable near the entrance region, and decrease gradually. The interfacial concentration demonstrates the same trend with the bulk liquid temperature. The concentration at the wall remains constant equal to inlet concentration at small downstream location, and decreases slowly because of the mass diffusion of water.

4.3. Local heat and mass transfer flux

Fig. 5(a) and (b) shows the variation of local mass and heat fluxes along the wall, respectively. The local heat fluxes at plate wall and at the interface are defined as follows:

$$q_w = -k \left(\frac{\partial T}{\partial y} \right)_{y=0}, \quad q_i = -k \left(\frac{\partial T}{\partial y} \right)_{y=\delta} \quad (9)$$

And the local mass flux at the interface as

$$m_i = -D\rho \left(\frac{\partial C}{\partial y} \right)_{y=\delta} \quad (10)$$

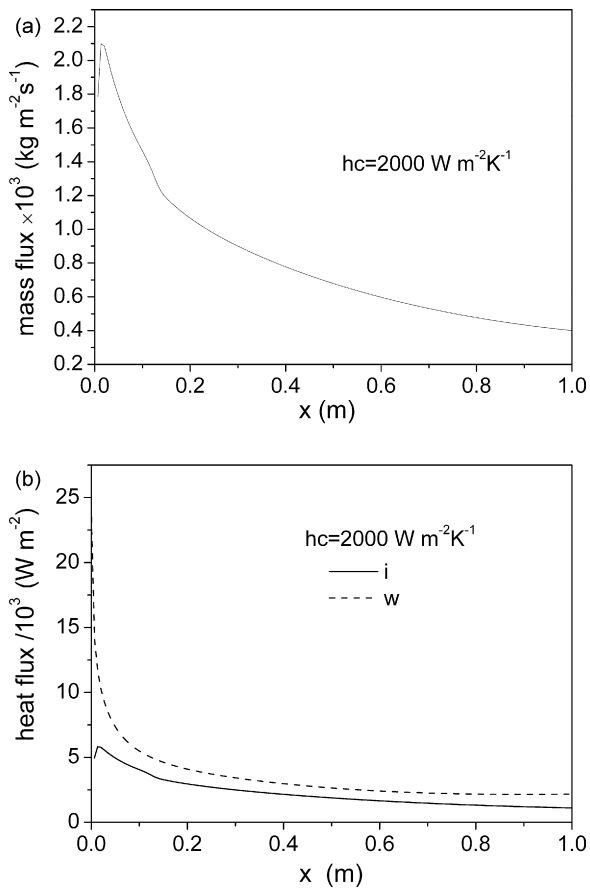


Fig. 5. The flux against downstream distance: (a) mass flux and (b) heat flux.

The heat and mass transfer fluxes at the interface are high near the inlet region, and then start to decrease after reaching their maximum values and decay gradually along the wall. As mentioned above, the LiBr solution is in thermodynamic equilibrium state at inlet. So the driving force of mass transfer is zero. After entering the absorber, because of remarkable effect of the cooling water, the temperature of liquid film decreases and the driving forces increase. So the vapor is absorbed into the film at the interface accompanying the release of absorption heat and heat and mass transfer fluxes increase. As the flowing downstream distance increases, the temperature difference between the film and the wall decreases and hence the heat flux at the wall decreases, leading to the heat and mass fluxes decreasing. Therefore, local maximums of heat and mass fluxes exist obviously. From Fig. 5, the maximum values for mass flux and heat flux are $2.1 \times 10^{-3} \text{ kg m}^{-2} \text{ s}^{-1}$ and $5.8 \times 10^3 \text{ W m}^{-2}$ corresponding to the location of $x = 13.2 \times 10^{-3} \text{ m}$, which is less than those of Yoon [8], due to the different wall boundary condition.

The local heat flux at the wall decreases rapidly after the inlet region and decreases slowly when $x > 0.1 \text{ m}$. It can be attributed to the change of the temperature difference between the bulk solution and the wall, as shown in Fig. 4(a).

As defined in Ref. [7], the absorption coefficient was introduced and calculated: $\varepsilon = (C_{in} - C_{out}) / (C_{in} - C_{min}) \times 100\%$. Where C_{out} is the bulk concentration at the outlet. C_{min} is the minimum concentration which can be determined when the bulk temperature of the solution at the outlet is equal to the inlet temperature of coolant. In the present simulation, ε is equal to 80%.

4.4. Effect of the physical properties

Most of the previous reports assumed constant physical properties. However, when the variable properties are incorporated into the analysis, the formulation and its programming became more complicated. In order to investigate the effect of physical properties on the absorption, the properties correlations, such as density, thermal conductivity and mass diffusivity, were selected from Ref. [17] and the dynamic viscosity was calculated from the correlation equation proposed by Lee et al. [18]. In the simulation procedure, udf was added to incorporate the simultaneous change of physical properties with concentration and temperature. The properties were calculated under the same inlet conditions for constant property case. The results for the cases of variable and constant properties are shown in Fig. 6. For this kind of coupled heat and mass transfer process, both thermal diffusivity and mass diffusivity play an important role. As the downstream distance increases, the temperature and concentration of solution decrease, leading to the increase of thermal diffusivity and the decrease of mass diffusivity. From Fig. 6(b), it can be seen that the interfacial temperature, bulk temperature and wall temperature are lower than those for constant property case. The thermal diffusivity increases as x increases, so heat is transferred more rapidly through the liquid film and the interface, and hence the bulk and wall temperatures decrease. When assumed that the thermodynamic equilibrium exists at the interface, the interfacial concentration decreases compared to the constant property case. But the low mass diffusivity restricts the diffusion of water at the interface into the film bulk. This gives rise to the higher bulk concentration and concentration at the wall for variable property case, as shown in Fig. 6(a). The typical local interfacial mass flux and heat flux along the wall are plotted in Fig. 7.

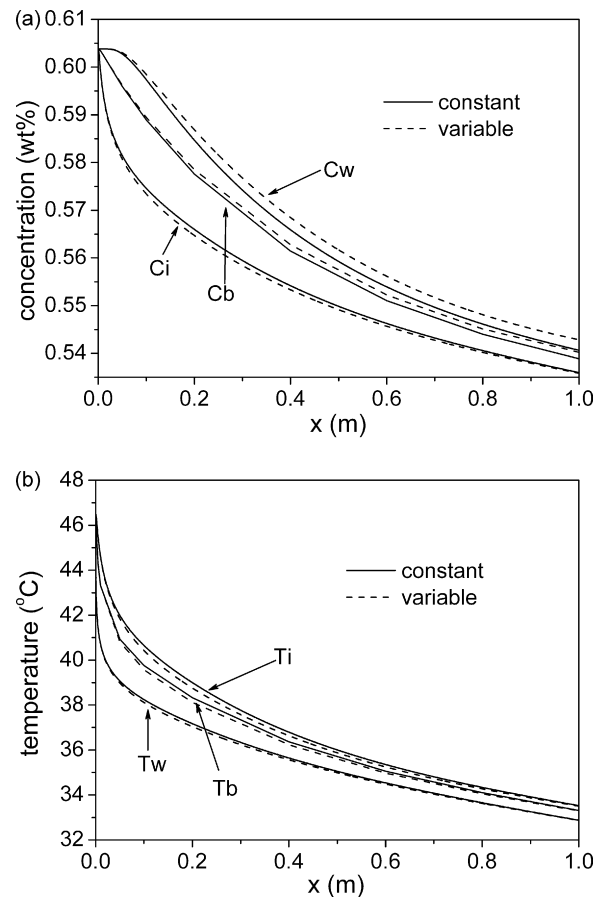


Fig. 6. The profile along the wall: (a) concentration and (b) temperature.

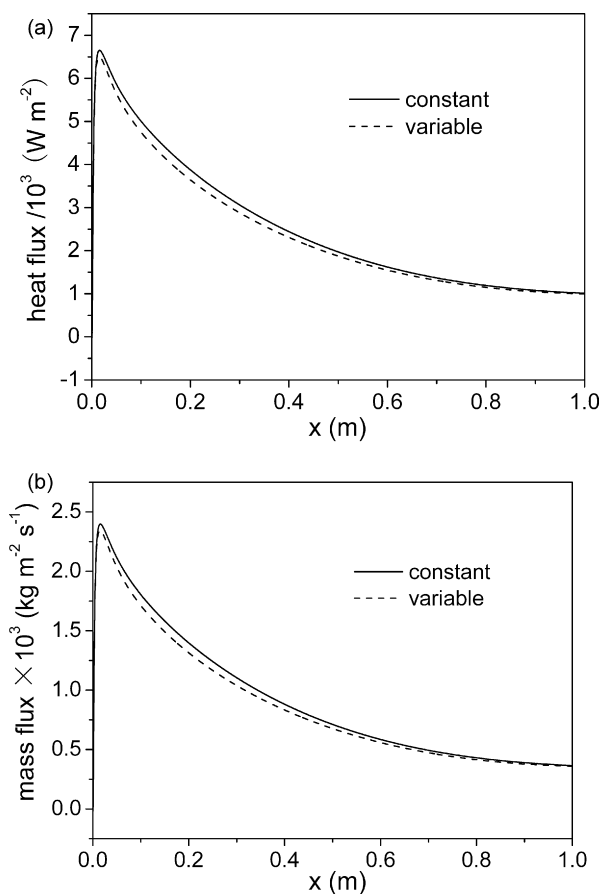


Fig. 7. The profile along the film: (a) heat flux and (b) mass flux.

From this figure, allowing for variable properties has little effect on local heat and mass fluxes near the inlet region. As the x increases, the local interfacial mass flux and heat flux with variable properties are slight lower than those for constant property case. According to the simulation results, the value of the total mass transfer rate of absorption is $1.686 \times 10^{-3} \text{ kg m}^{-1} \text{ s}^{-1}$ for constant property case and $1.576 \times 10^{-3} \text{ kg m}^{-1} \text{ s}^{-1}$ for variable property case, respectively, a decrease of 6.5%.

5. Conclusions

The combined heat and mass transfer process of liquid film falling outside a vertical tube during absorption of water vapor into a lithium bromide solution was numerically investigated using CFD software-Fluent. The more practical convective boundary condition in the cooling water side was considered. The heat transfer coefficient is assumed constant, but the coolant temperature changes linearly along its flow path. The results obtained can be summarized as follows.

The heat and mass transfer flux at the interface rise steeply after the inlet position, and then they start to decrease after reach-

ing respective maximum values and decay gradually along the downstream distance. The maximum values for mass flux and heat flux is $2.1 \times 10^{-3} \text{ kg m}^{-2} \text{ s}^{-1}$ and $5.8 \times 10^3 \text{ W m}^{-2}$ corresponding to $x = 13.2 \times 10^{-3} \text{ m}$.

Compared to the constant property case, although the temperature decreases, the total mass flux decreases. The prediction of the total absorption mass transfer rate is about 6.5% higher when assuming constant properties.

Acknowledgements

The authors are grateful for financial support by National High Technology Research and Development Program of China (863 Program), The National Natural Science Foundation of China (No. 50476072) and the Fund of New Century Excellent Talents in Universities of State Ministry Education of China (NCET-05-0280).

References

- [1] N.I. Grigoréva, V.E. Nakoryakov, Exact solution of combined heat- and mass-transfer problem during film absorption, *J. Eng. Phys. Thermophys.* 33 (1977) 1349–1353.
- [2] G. Grossman, Simultaneous heat and mass transfer in film absorption under laminar flow, *Int. J. Heat Mass Transfer* 26 (1983) 357–371.
- [3] N. Brauner, D.M. Maron, H. Meyerson, Coupled heat condensation and mass absorption with comparable concentrations of absorbate and absorbent, *Int. J. Heat Mass Transfer* 32 (1989) 1897–1906.
- [4] B.J.C. Van Der Wekken, R.H. Wassenaar, Simultaneous heat and mass transfer accompanying absorption in laminar flow over a cooled wall, *Int. J. Refrig.* 11 (1988) 70–77.
- [5] H.M. Habib, B.D. Wood, Simultaneous heat and mass transfer for a falling film absorber—the two phase flow problem, in: *Sol. Energy Eng. Proceedings of the 12th Annual International Solar Energy Conference*, ASME, 1990, pp. 61–67.
- [6] R. Yang, B.D. Wood, Numerical modeling of an absorption process on a liquid falling film, *Sol. Energy* 48 (1992) 195–198.
- [7] N. Kawae, T. Shigechi, K. Kanemaru, T. Yamada, Water vapor evaporation into laminar film flow of a lithium bromide-water solution (influence of variable properties and inlet film thickness on absorption mass transfer rate), *Heat Transfer—Jpn. Res.* 18 (1989) 58–70.
- [8] J.I. Yoon, T.T. Phan, C.G. Moon, P. Bansal, Numerical study on heat and mass transfer characteristic of plate absorber, *Appl. Therm. Eng.* 25 (2005) 2219–2235.
- [9] A. Yigit, A numerical study of heat and mass transfer in falling film absorber, *Int. Commun. Heat Mass Transfer* 26 (1999) 269–278.
- [10] I. Morioka, M. Kiyota, Absorption of water vapor into a wavy film of an aqueous solution of LiBr, *JSMI Int. J., Series 2* 34 (1991) 183–188.
- [11] R. Yang, D. Jou, Heat and mass transfer of the wavy film absorption process, *Can. J. Chem. Eng.* 71 (1993) 533–538.
- [12] V. Patnaik, H. Perez-Blanco, A study of absorption enhancement by wavy film flows, *Int. J. Heat Fluid Flow* 17 (1996) 71–77.
- [13] H. Sabir, K.O. Suen, G.A. Vinnicombe, Investigation of effects of wave motion on the performance of a falling film absorber, *Int. J. Heat Mass Transfer* 39 (1996) 2463–2472.
- [14] G. Grossman, M.T. Heath, Simultaneous heat and mass transfer in absorption of gases in turbulent liquid films, *Int. J. Heat Mass Transfer* 27 (1984) 2365–2376.
- [15] W.A. Miller, M. Keyhani, The correlation of simultaneous heat and mass transfer experimental data for aqueous lithium bromide vertical falling film absorption, *J. Sol. Energy Eng.-Trans. ASME* 123 (2001) 30–42.
- [16] L.A. McNeely, Thermodynamic properties of aqueous solutions of lithium bromide, *ASHRAE Trans.* 85 (1979) 413–434.
- [17] J.W. Andberg, Absorption of vapors into liquid films flowing over cooled horizontal tubes. Ph.D. thesis, Mech. Eng., University of Texas, Austin, Appendix D, 1986.
- [18] R.J. Lee, R.M. DiGiulio, S.M. Jetter, A.S. Teja, Properties of lithium bromide-water solutions at high temperatures and concentrations-II: density and viscosity, *ASHRAE Trans.* 96 (1990) 709–728.